Chemical State of Iron of LiFePO$_4$ during Charge-Discharge Cycles Studied by *In-Situ* X-ray Absorption Spectroscopy

Katsuya Inoue, Shun Fujieda, Kozo Shinoda, Shigeru Suzuki* and Yoshio Waseda

Institute of Multidisciplinary Research for Advanced Materials, Tohoku University, Sendai 980-8577, Japan

In-situ X-ray absorption spectroscopy (XAS) at the Fe K-edge X-ray absorption near edge was used to investigate the chemical change of LiFePO$_4$, which is a candidate cathode material for lithium ion batteries, during charge-discharge cycles. The relative amount of FePO$_4$ formed in the LiFePO$_4$ by the charge-discharge cycles was estimated from the XAS spectra. The results show that the amount of FePO$_4$ in the LiFePO$_4$ increased with charging and decreased with discharging. While a linear relationship between the relative amount of FePO$_4$ and electrical capacity was observed during the initial charging, it deviated from linearity during the charge-discharge cycles. This may be attributed to the irreversible diffusion paths of lithium ions and/or the partial formation of inactive FePO$_4$ in the LiFePO$_4$ during the charge-discharge cycles. It is shown that *in-situ* XAS has sufficient potential to nondestructively characterize heterogeneous electrochemical reactions in electrode materials during charge-discharge cycles. [doi:10.2320/matertrans.M2010229]

1. Introduction

Olivine-type LiFePO$_4$, first proposed in 1997, is one of the promising electrode materials for Li-ion batteries.[1] This material has a relatively large theoretical capacity of 170 mAhg^{-1} and a potential of ca. 3.4 V against Li$^+$/Li. It is not composed of valuable or toxic elements. Although it exhibits good thermal stability in the fully charged state, it has a relatively low electrical conductivity, which restricts the rate of Li$^+$ intercalation/deintercalation.[2,3] In order to investigate the structural changes in LiFePO$_4$ by Li$^+$ intercalation/deintercalation, Rietveld refinement of the X-ray or neutron diffraction patterns and Mössbauer spectroscopy were used.[4,5] The results showed that the atomic coordination and lattice parameters of the structure, as well as the chemical state of the iron, are changed by the formation of FePO$_4$ in the LiFePO$_4$. However, it is often necessary to measure the chemical change of LiFePO$_4$ during charge-discharge cycles *in-situ*, because it takes a long time to obtain high-quality data using X-ray or neutron diffraction and Mössbauer spectroscopy.

X-ray absorption spectroscopy (XAS) using synchrotron radiation is useful for investigating the chemical state and local structure of an element of interest present in a sample.[6,7] The X-ray absorption near edge structure (XANES) is sensitive to the valence of an element present in a sample, and provides information about small changes in the chemical state of a specific element in a sample. *In-situ* XAS analysis may be useful for non-destructively characterizing the chemical state of a specific element in electrochemical reactions. Actually, the chemical state and local structure of a cathode material have sometimes been studied using *in-situ* XAS.[8,9] However, the structural changes in these materials during cyclic charging-discharging have not been sufficiently studied because of the difficulty of characterizing samples with various microstructures. The objective

of this study was to characterize the chemical state of Fe in LiFePO$_4$ during charge-discharge cycles using *in-situ* XAS analysis. We focused on the irreversible diffusion process during cyclic charging-discharging.

2. Experimental

2.1 Sample preparation

Particle samples of LiFePO$_4$ were obtained by the solid-state reaction of a stoichiometric amount of Fe$_3$(PO$_4$)$_2$·nH$_2$O—prepared in aqueous solution—with Li$_3$PO$_4$.[10] In order to prepare particles of Fe$_3$(PO$_4$)$_2$·nH$_2$O, an aqueous solution of sodium hydroxide (NaOH) was added to one containing ferrous sulfate n-hydrate (FeSO$_4$·nH$_2$O) and one of phosphoric acid (H$_3$PO$_4$) in a reaction vessel at 25°C. The precipitated particles of Fe$_3$(PO$_4$)$_2$·nH$_2$O were washed with Ar-bubbled water by centrifugation, and then separated by the freeze-drying method. Particles of Fe$_3$(PO$_4$)$_2$·nH$_2$O were then mixed with particles of Li$_3$PO$_4$ and 20 mass% ascorbic acid. After the mixture was heated at 350°C for 3 h under Ar-10%H$_2$ gas, it was ground at room temperature. Finally, it was annealed at 600°C for 5 h. The structure of the synthesized LiFePO$_4$ was identified by X-ray diffraction. A cathode was prepared by spreading a mixture of LiFePO$_4$, acetylene carbon black powder, and polyvinylidene fluoride (ratio 85 : 10 : 5) with N-methylpyrrolidone onto an aluminum foil. After the cathode was dried at 120°C, it was pressed and cut into a round sheet. A cell for measurements was assembled with the lithium metal anode and electrolyte in an argon-filled glove box. The electrolyte used was 1 M LiPF$_6$ in ethylene carbonate and diethyl carbonate (1 : 1 in volume).

2.2 Measurements

The crystallographic structure of the particles was identified by X-ray diffraction (XRD) using Cu Kα radiation. The morphologies of the particles were observed using a scanning electron microscope (SEM, HITACHI S-4100L). A cell was

---

*Corresponding author, E-mail: ssuzuki@tagen.tohoku.ac.jp
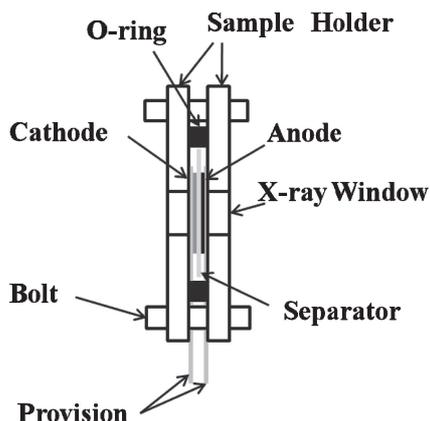
Fig. 1 *In-situ* cell for XAS measurements.

Fig. 2 XRD patterns from sample. The reference line for the olivine type LiFePO$_4$ provided in the JCPDS database is also shown.

designed for *in-situ* XAS measurement using synchrotron radiation, as shown in Fig. 1. The cell package consisted of the anode, cathode, Celgard separator, and electrolyte. Provisions for current measurements were sandwiched by thin sheets of stainless steel. The cell was assembled under an argon atmosphere in a glove box. The charge/discharge of the cell was cycled galvanostatically at a rate of 0.5 C (1 C = 170 mAh/g) in a voltage range of 2.5–4.2 V against Li at room temperature. *In-situ* XAS measurements were performed in the transmission mode using the high-brilliance synchrotron radiation of beamline BL01B1 at SPring-8 of the Japan Synchrotron Radiation Research Institute, Japan. The XAS spectra for the X-ray absorption near edge structure (XANES) at the Fe K-edge were obtained for approximately 1 min. After the spectral backgrounds were subtracted, the relative amounts of FePO$_4$ formed in the LiFePO$_4$ were estimated from the XANES spectra using Rigaku REX2000 software.

3. Results and Discussion

The XRD pattern of a sample synthesized by the present method is shown in Fig. 2, together with the JCPDS data for olivine type LiFePO$_4$ as a reference sample. All of the diffraction peaks are assigned to the orthorhombic olivine type LiFePO$_4$. The LiFePO$_4$ particles synthesized in this study exhibited relatively good crystallinity, as observed by the sharp diffraction peaks.

SEM images of the LiFePO$_4$ particles are shown in Fig. 3. The particles were sub-micron in size, and island-like carbon particles were observed on the surface of the LiFePO$_4$ particles. The charge-discharge properties of the electrode may be affected by the particle size morphology and carbon coating. As the particles prepared in this study revealed size distributions and carbon coatings that did not cover the particles, this may be the reason that the electrical capacity of the sample was about 60% of the theoretical value, as discussed later.

Figure 4 shows the voltage versus capacity of the as-prepared LiFePO$_4$ for up to 4.2 V during the first galvanostatic charging and discharging at a rate of 0.5 C. A voltage plateau at approximately 3.6 V, which appeared to be deviated from the ideal redox voltage due to experimental
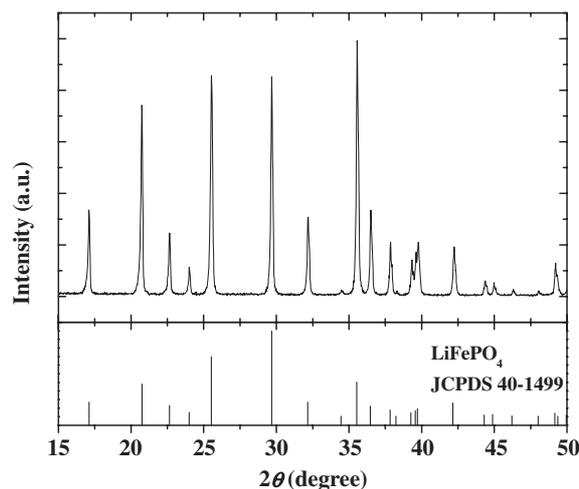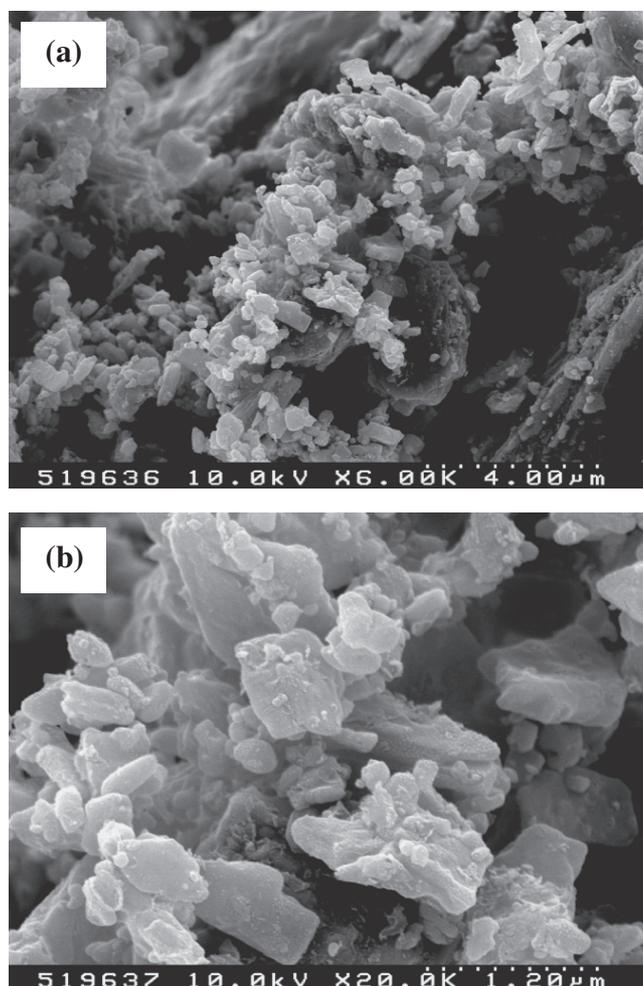
Fig. 3 SEM images of LiFePO$_4$ particles. The magnification in Fig. 3(b) is larger than that in Fig. 3(a).

conditions, was observed for up to approximately 60 mAhg^{-1}. The nominal capacity during the initial charging was 98 mAhg^{-1}. The fact that the high voltage and electrical capacity are lower than the theoretical values may be attributed primarily to the heterogeneity of the sample. The

K. Inoue, S. Fujieda, K. Shinoda, S. Suzuki and Y. Waseda
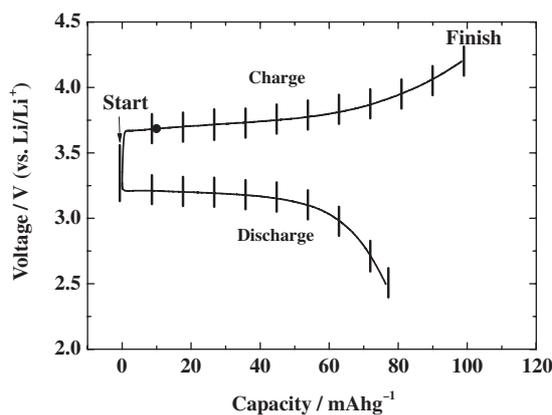
Fig. 4 Initial charging curves for LiFePO$_4$ at $85\,\mathrm{mAg^{-1}}$. The marked numbers show the instances at which *in-situ* XAS measurements were performed.

changes in the electrical capacity with discharging are also shown in Fig. 4. The discharging curve is not symmetric to the charging curve, which may be because of the irreversible diffusion of lithium ions in this sample, heterogeneities of the carbon coating on the LiFePO$_4$ particle surfaces, LiFePO$_4$ particle size, etc., as shown in Fig. 3. In this study, the charge-discharge characteristics were compared with the amounts of FePO$_4$ formed in the LiFePO$_4$ during charge-discharge cycles using non-destructive *in-situ* XAS measurements. In order to characterize the relation between the charging and the chemical state of the iron, *in-situ* XAS measurements were carried out at the capacities marked on the curves.

The XANES spectra taken at the Fe K-edge for LiFePO$_4$ during the initial charging and discharging are shown in Figs. 5(a) and (b), respectively. It took one min for each XAS measurement, and the time intervals between the measurements were constant. The position of the Fe K-edge in the XANES spectra systematically shifted toward the higher energy side. The position of the absorption edge for a ferrous compound is generally located at the low energy side compared to that for a ferric compound, although the spectra include more information about the local electric states of iron.[5] These systematic shifts in the edge position with charging indicate the continuous chemical change of Fe(II) into Fe(III) caused by the deintercalation of lithium ions in the LiFePO$_4$, that is, the formation of FePO$_4$. The XANES spectra obtained during discharging showed that Fe(III) changed back into Fe(II) in the LiFePO$_4$, although the spectra were not completely reversible. This may correspond to the result of the low discharge capacity compared to the charge capacity, as shown in Fig. 1. Because information about the structures of LiFePO$_4$ and FePO$_4$ is contained in these Fe K-edge XANES spectra, the LiFePO$_4$/FePO$_4$ molar ratio can be estimated from them.

The XANES data were collected in the form of the X-ray absorption coefficient (μ) versus energy (E). XANES data for a sample mixture consisting of LiFePO$_4$/FePO$_4$ were obtained from the data for homogeneous LiFePO$_4$ and FePO$_4$ samples using the following relationship:

$$\mu(E)_{\mathrm{LiFePO_4/FePO_4}} = f_{\mathrm{LiFePO_4}}\mu(E)_{\mathrm{LiFePO_4}} + f_{\mathrm{FePO_4}}\mu(E)_{\mathrm{FePO_4}},$$
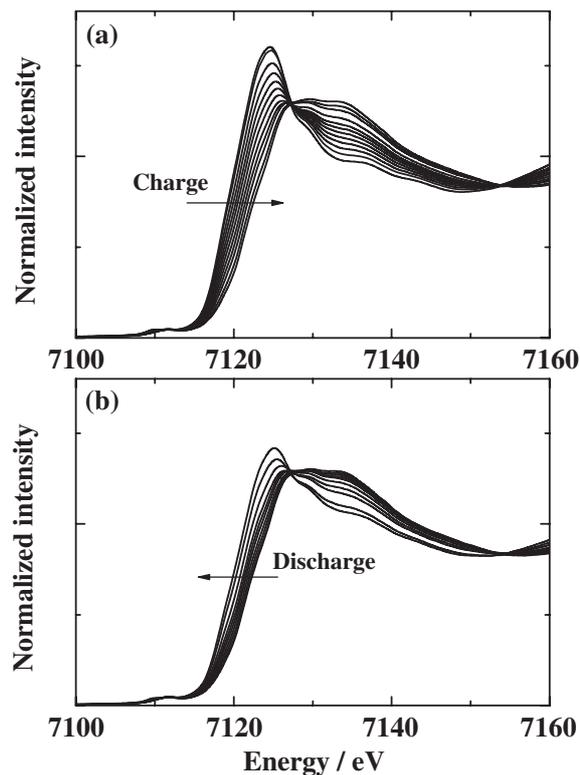
Fig. 5 Normalized XANES spectra of LiFePO$_4$ at Fe K-edge during initial charging. The spectra were measured at the points marked with the same colors in Fig. 1.

where f_i is the fraction of component i in the LiFePO$_4$/FePO$_4$ sample mixture and $f_{\mathrm{LiFePO_4}} + f_{\mathrm{FePO_4}} = 1$. However, as the FePO$_4$ XANES spectrum was not practically available in this study, LiFePO$_4$ remained in the sample was estimated to be the final capacity. Therefore, the relative amount of FePO$_4$ formed in the LiFePO$_4$ during the initial charging was estimated using the following relation:

$$\mu(E)_{(i)} = f_{\mathrm{(Start)}}{}^i \mu(E)_{\mathrm{(Start)}} + f_{\mathrm{(Finish)}}{}^i \mu(E)_{\mathrm{(Finish)}},$$

where i is the fraction of component i at each capacity denoted in Fig. 1, $f_{\mathrm{(Start)}}{}^i + f_{\mathrm{(Finish)}}{}^i = 1$, and $f_{\mathrm{(Finish)}}{}^i$ indicates the relative amount of FePO$_4$.

Figure 6 shows the relative amount of FePO$_4$ estimated from the XANES spectra as a function of the relative electrical capacity in the initial charge and discharge. The amount of FePO$_4$ formed in the LiFePO$_4$ and the nominal capacity during the initial charging are considered to be 100%. The colors of the marks correspond to the colors of the marks on the initial charging and discharging curves in Figs. 4(a) and (b). The formation of FePO$_4$ in the LiFePO$_4$ theoretically corresponds to an electrical charge. Although the relative amount of FePO$_4$ increased linearly with the relative amount of electrical capacity during the initial charging, the linear relationship was not maintained during the subsequent discharging. This suggests that the intercalation of lithium ions in FePO$_4$ is considerably influenced by some microstructural changes in the samples by the deintercalation of lithium ions in LiFePO$_4$ during the initial charging.

The relationship between the relative amount of FePO$_4$ and the relative capacity obtained over several cycles is
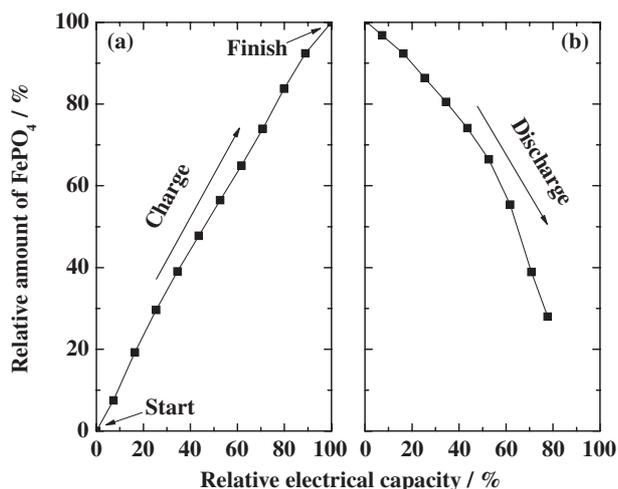
Fig. 6 Relative amount of FePO₄ as a function of relative electrical capacity during initial charging.
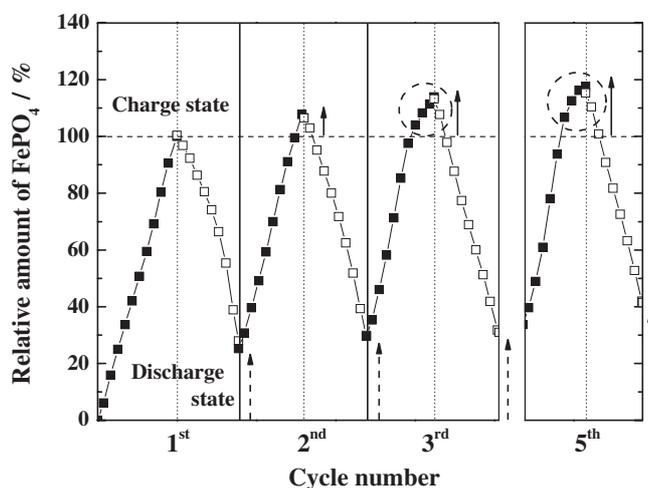
Fig. 7 Relative amount of FePO₄ as a function of relative electrical capacity in subsequent charge-discharge cycles.

shown in Fig. 7, where the solid and open marks denote data measured during charging and discharging, respectively. The results of the first cycle in Fig. 6 are plotted in the first cycle of Fig. 7. The relative amount of FePO₄ was considered to be 100% after the initial charging. Andersson *et al.* reported the inactive LiFePO₄ and remnant FePO₄ formed during the first charge-discharge cycles.[5] In this study, the amount of FePO₄ gradually increased with the charge-discharge cycles. These results indicate that portions of the LiFePO₄, which did not contribute to the deintercalation during the initial charging, gradually contributed to the electrochemical reaction of deintercalation. During discharging, the FePO₄ formed in the LiFePO₄ was not all reversibly transformed back into LiFePO₄, but a remnant amount of FePO₄ was left. This tendency progressively changed. These results suggest that the FePO₄ transformed from LiFePO₄ was gradually stabilized, and that the inactive FePO₄ gradually formed during charge-discharge cycles. In this way, the capacity gradually decreased during the charge-discharge cycles. We were able to characterize

the local chemical change of LiFePO₄ during the charge-discharge cycles.

It is worth noting that the electrical capacity was gradually reduced during the charge-discharge cycles. This may have resulted from a decrease in active LiFePO₄ and an increase in inactive FePO₄. In addition, the relationship between the relative amount of FePO₄ and the electrical capacity exhibited large non-linearities in the third and fifth cycles, which are circled by broken lines in Fig. 7. These non-linearities indicate that the deintercalation reactions in the LiFePO₄ were prevented despite the charging process. This phenomenon could have occurred because of the inhomogeneous carbon coating on the particle surfaces, the formation of cracks,[11] defects, and the exchange of Fe ions in octahedral 4c sites with Li ions in 4a sites during the charge-discharge cycles, as in the case of LiNiO₂.[12] The Li motion in the LiFePO₄ is particularly susceptible to blockage by defects and impurities.[13] It is difficult to identify the exact reason. Nevertheless, the present results suggest that *in-situ* XAS analysis is effective at nondestructively characterizing the chemical state of iron in cathode materials such as LiFePO₄, even though small amounts of hardly detected components may also contribute to the electrochemical reactions.

4. Conclusions

Systematic shifts in the position of the Fe K-edge XANES spectra were observed in electrochemically charged LiFePO₄ in an electrochemical cell. These shifts corresponded to the local change of LiFePO₄ into FePO₄ through the deintercalation of lithium ions. The relative amount of FePO₄ estimated from XANES spectra was linearly related to the capacity change during the initial charging. However, this relationship gradually deviated from linearity during subsequent charge-discharge cycles. This implies that the amount of inactive LiFePO₄ increased during the charge-discharge cycles. It was demonstrated that *in-situ* X-ray absorption spectroscopy shows sufficient potential for nondestructively characterizing the relationship between the chemical state of metal elements in LiFePO₄ and the electrical capacity of an electrode during cyclic electrochemical operations.

REFERENCES

1) A. K. Padhi, K. S. Nanjundaswamy and J. B. Goodenough: J. Electrochem. Soc. **144** (1997) 1188–1194.
2) A. K. Padhi, K. S. Nanjundaswamy, C. Masquelier, S. Okada and J. B.

Goodenough: J. Electrochem. Soc. **144** (1997) 1609–1613.

3) S. Franger, F. Le Crase, C. Bourbon and H. Rouault: Electrochem Solid-State Lett. **5** (2002) A231–A233.

4) A. S. Andersson, B. Kalska, L. Häggström and J. O. Thomas: Solid State Ionics **130** (2000) 41–52.

5) A. S. Andersson and J. O. Thomas: J. Power Sources **97–98** (2001) 498–502.

6) O. Haas, A. Deb, E. J. Cairns and A. Wokaun: J. Electrochem. Soc. **152** (2005) A191–196.

7) L. Laffont, C. Delacourt, P. Gibot, M. Y. Wu, P. Kooyman, C. Masquelier and J. M. Tarascon: Chem. Mater. **18** (2006) 5520–5529.

8) A. Deb, U. Bergmann, E. J. Cairns and S. P. Cramer: Electrochim. Acta **50** (2005) 5200–5207.

9) K.-W. Nam, X.-J. Wang, W.-S. Yoon, H. Li, X. Huang, O. Haas, J. Bai and X.-O. Yang: Electrochem. Commun. **11** (2009) 913–916.

10) M. Herstedt, M. Stjerndahl, A. Nytén, T. Gustafsson, H. Rensmo, H. Siegbahn, N. Ravet, M. Armand, J. Thomas and K. Edström: Electrochem. Solid-State Lett. **6** (2003) A202–A206.

11) D. Wang, X. Wu, Z. Wang and L. Chen: J. Power Sources **140** (2005) 125–128.

12) P. Kalyani and N. Kalaiselvi: Sci. Tech. Adv. Mater. **6** (2005) 689–703.

13) D. Morgan, A. Van der Van and G. Ceder: Electrochem. Solid-State Lett. **7** (2004) A30–A32.